Title	Network topological effects on the macroscopic Bureau of Public Roads function
Author(s)	Wong, W; Wong, SC
Citation	Transportmetrica A: Transport Science, 2016, v. 12 n. 3, p. 272-296
Issued Date	2016
URL	http://hdl.handle.net/10722/223204
Rights	This is an Accepted Manuscript of an article published by Taylor & Francis in Transportmetrica A: Transport Science on 29 Jan 2016, available online: http://wwww.tandfonline.com/10.1080/23249935.2015.1129650; This work is licensed under a Creative Commons Attribution-NonCommercial-NoDerivatives 4.0 International License.

Network Topological Effects on the Macroscopic Bureau of Public Roads Function

Wai Wong and S.C. Wong

Department of Civil Engineering, The University of Hong Kong, Pokfulam, Hong Kong

Abstract

Cost flow functions are a central class of models in the transport field because they are an essential ingredient of static user equilibrium traffic assignment and transport policy and planning analysis. Macroscopic cost flow (MCF) functions, which model travel cost at different levels of network use, have gained much attention in recent decades due to their potential applications in area-wide traffic management and control, and initial land use planning. They are the collective outcomes of the responses of road users to the existing transportation network and the interactions between road users at different levels of traffic demand. Network topological effects have long been anticipated to be the primary factors governing the shape and performance of a network. However, few studies have investigated network topology. This paper aims to unveil the direct link between network topological metrics and the parameters of a specific MCF, in the form of macroscopic Bureau of Public Roads (MBPR) function, with the support of real-world data. Seventy one 1 km × 1 km urban built-up regions were sampled in Hong Kong. The MBPR functions of the selected regions were calibrated using taxi global positioning system data. Intensive investigations revealed that the average number of junctions per unit distance and the road density were topological features correlating with the free-flow travel time and congestion sensitivity parameters of the MBPR function, respectively. A spatially variable MBPR (SVMBPR) function was established.

Keywords: Cost Flow Function; Network Topological Effects; Macroscopic Bureau of Public Roads Function; GPS

1. Introduction

Cost flow functions, also known as volume delay functions, express travel cost as a function of traffic demand. They are the result of the interactions between transportation infrastructure, road users, and traffic management and control schemes at different levels of transport system use. Monotonically increasing relationship models have been used to represent the increase in travel time required for a trip due to congestion as the volume of traffic and interactions between vehicles increase. These are an important class of transport models as they are the essential input for the standard mathematical programing formulation in static traffic assignment problems (Sheffi, 1985; Patriksson, 1994). Compared to dynamic models, static models do not include the temporal dimension and capture the traffic congestion dynamics, but are useful simplifications for steady-state analysis because static models are generally less computationally demanding and relatively easy for implementation. A cost flow function can

generally be classified as a link-based model, in which only a road segment is taken into account, or an area-based model, describing a network-wide cost flow relationship over a region.

Various link-based performance functions have been proposed and used in practice (Branston, 1976). Exponential cost flow functions (Schneider, 1963; Smock, 1963; Overgaard, 1967) were the earliest proposed models. However, their use was not widespread due to the superiority of other functional forms over the exponential form (Klieman et al., 2011). In contrast, the Bureau of Public Roads (BPR) function (Bureau of Public Roads, 1964) and Davidson's function (Davidson, 1966), which were also proposed in the 1960s, have received much more attention and have attracted intensive discussion since their introduction. The BPR function is based on fitting data obtained from an uninterrupted freeway. This polynomial cost flow function is now used in the Highway Capacity Manual (Transportation Research Board, 2000) and in many European countries and the United States (Dowling et al., 1998; Lum et al., 1998). It also plays a crucial role in static user equilibrium analysis (García-Ródenas and Verastegui-Rayo, 2013). Despite its prevalence due to its simplicity, Spiess (1990) identified intrinsic deficiencies in using the BPR function for traffic assignment and proposed the conical volume-delay function as an alternative. This proposed function satisfies the seven stated desirable requirements of a cost flow function to solve the problem of slow convergence due to a large volume to capacity ratio during the first few iterations, guarantees the uniqueness of assigned traffic flow, and reduces the computational time (Spiess, 1990).

Davidson's function (Davidson, 1966) was derived from queuing theory and has gained some popularity since it was proposed. Taylor (1977) proposed a method for estimating the parameters in Davidson's model and explored the sensitivity and reliability of the estimated parameters. However, the inherent inconsistency of its parameter definition, which implies that the flow capacity and the reciprocal of the free-flow travel time are equal, has aroused considerable discussion (Golding, 1977). Davidson (1978) modified the function and attempted to redefine the delay parameter to remove this inconsistency. But the modification led to another inconsistent parameter, implying better service quality with increased free-flow travel time (Akçelik, 1991). Davidson's function was further modified to obtain a finite travel time around the capacity flow (Akçelik, 1978; Akçelik, 1981). Taylor (1984) described a network equilibrium assignment using the modified Davidson's function. Tisato (1991) nevertheless reported that this modified version may possess potential deficiencies because the slope of the linear extension behaved poorly as the delay parameter, known as the service quality parameter, approached its limit of one. In response, Akçelik (1991) derived a time-dependent form of Davidson's function using coordinate transformations to address both the issue of inconsistent parameter definitions and the possibility of travel time overestimation around the capacity flow caused by the modification proposed by Tisato (1991). An extension of Akçelik's function is used in the Highway Capacity Manual (Transportation Research Board, 2000). In addition to these most commonly used cost flow functions, other model forms have also been proposed. Examples include a volume delay function allowing bigger trip matrices to be assigned without over-assignment (Jastrzebski, 2000) and a new delay model that was developed for unsignalized

intersections based on video and vehicle license plate data (Shahpar et al., 2011). Other models such as the Singapore model proposed by Xie, Cheu, and Lee (2011) and the Skabardonic-Dowling model (Skabardonic and Dowling, 1997) have considered the effects of traffic signals in their estimations of speed and travel time on arterials. Davis and Xiong (2007) also provided a useful review of these cost flow functions.

Accurate cost flow function model calibration is essential for reliable steady-state analysis. Researchers have continued trying to advance the calibration methods and calibrating cost flow functions using real-world data to obtain more accurate and reliable models that reflect reality. Cetin et al. (2012) proposed a method based on a genetic algorithm for calibrating the optimal and consistent model parameters of cost flow functions. Regimes exceeding their capacity are normally unobservable. However, freeway detector data from bottlenecks and queuing analysis have recently been used to calibrate cost flow functions with traffic demand exceeding its capacity by measuring the demand at oversaturated signalized junctions (Huntsinger and Rouphail, 2011). Archived public data have also been used to calibrate the most commonly used cost flow functions and to study the suitability of modeling link performance with different facility types using these volume delay functions (Mtoi and Moses, 2014).

Area-based cost flow functions, known as macroscopic cost flow (MCF) functions, depict the travel time and traffic demand relationship associated with a network-wide region. MCFs help planners and engineers to understand how road users and the road network interact with each other at different traffic demand levels. Using MCFs to analyze and plan complex urban networks has several advantages over link-based cost flow functions. For instance, they substantially reduce the problem size and computational analysis time because the travel time and traffic demand relationship over a region can be modelled by a single MCF instead of a set of link-based cost flow functions for each link within the region. MCFs can be used for policy analysis, network management schemes, and land use policy development (Liu et al., 2011). They are also the essential inputs of continuum modeling for urban cities for a number of applications, such as macroscopic user equilibrium problems (Wong, 1998; Wong et al., 1998; Ho et al., 2007; Ho et al., 2004; Ho et al., 2006), congestion-pricing problems (Ho et al., 2005; Ho et al., 2013b), market areas of competitive facilities (Wong and Yang, 1999; Yang and Wong, 2000), network vulnerability analysis (Ho et al., 2013a), facility location problems (Wong and Sun, 2001), housing allocation problems (Ho and Wong, 2007), and, more specifically, optimal housing patterns for minimal traffic emissions (Yin et al., 2013; Yin et al., 2012). In addition to reducing the computational time, approximating a dense urban network as a continuum requires a smaller data input and provides a better understanding of the network characteristics on a global scale (Ho and Wong, 2006). However, the existence of a macroscopic relationship between travel time and traffic demand, and a sophisticated method for calibrating MCF models based on real-world data, are essential for the application of continuum models.

The appealing potential benefits of MCF applications in traffic management policy analysis and land use planning have driven researchers to devote much effort to extending cost flow functions from link-based to area-based. Many researchers have attempted to

develop network-wide speed-flow relationships (Thomson, 1967; Wardrop, 1968; Ohta and Harata, 1989). Recently, May et al. (2000) confirmed that generating an area-wide speed-flow relationship based on a simulation was possible. They found that an MCF, which was essential for the estimation of network traffic demand, differed from the performance curve generated from a macroscopic fundamental diagram (MFD), which possessed a backward-bending relationship between speed and traffic flow. The difference was demonstrated using a micro-simulation model, NEMIS, based on a hypothetical grid network and a ring radial network. Liu et al. (2011) pointed out that the (mis)use of the performance curve generated from an MFD to estimate traffic demand would seriously underestimate the traffic demand and cost of congestion for steady-state analysis. Based on the results from a micro-simulation model, DRACULA, Liu et al. (2011) also investigated how the temporal and spatial distribution and origin-destination movements within a network affected the shapes of MCFs. However, these studies were based on simulations and lacked the support of empirical data. Wong and Wong (2015) studied the removal of systematic bias from model calibration due to the variability arising from a linear data projection. They used a combination of real-world global positioning system (GPS) data and data from on-road fixed detectors to calibrate the macroscopic BPR (MBPR) function and confirmed that the macroscopic relationship between travel cost and traffic demand did indeed exist.

MCFs are the result of the aggregated responses of road users toward the existing road network, according to its topological features. A network's topology is therefore closely related to its performance and is the primary factor governing the shape of the MCF. It is therefore important to understand the effects of network topological features on MCFs to further improve network performance. A limited number of studies on the effects of topological features on the performance of link have been conducted since the 1960s. Smeed (1966) studied the relationship between the road capacity of central London and both the town area and road density. Wardrop (1968) investigated how the width of a road, the number of controlled intersections per mile, and the proportion of green time affected the average speed of vehicles running on a road in a link-based study. Simulation results have shown that the shape of an MCF of a grid network is less sensitive to changes in the origin-destination pattern than a ring-radial network (May et al., 2000). Although Liu et al. (2011) mentioned that the shapes of MCFs depend on the nature of the network, the effects of network characteristics on MCFs have not been investigated explicitly. Therefore, the effects of network topological features on network performance (i.e., the shape of the MCFs) remain unknown.

This study aimed to fill the aforementioned research gap and extend our knowledge of the relationships between network topological features and the shapes of MCFs. Seventy one 1 km x 1 km regions with various topological features in the highly urbanized regions of Hong Kong were sampled. The MCFs of these selected regions were calibrated using real-world taxi GPS data. The MBPR function was used as the MCF. The MBPR function is algebraically tractable, and its relatively simple parameter definitions are appealing to MCF applications. A number of potential topological metrics of the selected regions were extracted with commonly used geographic information system (GIS) software. The relationships

between the topological features and the parameters of the MBPR were established. We developed the spatially variable MBPR (SVMBPR) function, which can estimate the MBPR function and the performance of any network over a region using only network topological data. Compared with the relatively time-consuming and costly traffic data collection and processing, network topological data can be more readily obtained from online maps via image processing. The developed function can provide planners with insights into how topological characteristics affect the performance of a transport network and estimate the MBPR functions of networks serving as the inputs of continuum modeling.

The remainder of the paper is organized as follows. Section 2 describes the sampling criteria and sampled regions of highly urbanized areas in Hong Kong. Section 3 presents the traffic data required for the model calibration and summarizes the model calibration results. After introducing the potential topological metrics, an in-depth analysis of the effects of network topological features on the shape of the MBPR and developed SVMBPR functions are presented in Section 4. Section 5 summarizes the findings and discusses potential future research directions.

2. Sampled sites description

Hong Kong is one of the leading global financial centers. It is also one of the most densely populated cities, with a population of over seven million people living on about one thousand square kilometers of land. Its limited land has turned Hong Kong into one of the most vertical cities in the world. Dense road networks serve as the backbone and skeleton of the city. These networks have different topological features and are essential to the city. They have been built along the coastal area of Hong Kong Island and all over Kowloon and the new towns in the New Territories to ensure the efficient movement of goods and people.

We sampled networks with different topological features to establish the relationship between the networks' topological features and the shape of the selected MCF. The major sampling criteria for the studied networks are listed as follows.

- The sampled networks had to cover as many urban areas as possible, such that a full range of relationships between their topological metrics and the parameters of the chosen MCF could be established.
- Each sampled network had to be as homogeneous as possible. To achieve this, the sampling grid had to be as small as possible. However, due to the resolution of the available GPS data recorded twice in a minute (discussed in Section 3.2) and the maximum free-flow speed of around 80 km/h in Hong Kong, the maximum distance travelled by a vehicle in 30 seconds was about 0.67 km. Thus, a 1 km × 1 km sampling grid was chosen to capture the traffic information of the GPS-equipped vehicles and minimize the chance of sampling a highly heterogeneous network.
- A sampled network had to include as many Annual Traffic Census (ATC) stations as possible to ensure the estimated sample mean and variance of the scaling factor (see

Section 3.3 and a study by Wong and Wong (2015)) for the data projection and model calibration were accurate and reliable.

- The overlapping area of any two sampled networks had to be kept as small as possible, such that each sampled network possessed its major distinct and unique topological features.
- Where possible, no boundary of a sampled network was permitted to run along the centerline of a road or cut across a junction.

Seventy one 1 km × 1 km regions covering most of the densely built-up regions of Hong Kong were sampled in accordance with the aforementioned sampling criteria, as shown in Figure 1. The selected studied regions possessed very diverse land use patterns, including the central business district (CBD) with numerous high-rise buildings and offices, a highly dense commercial and residential mixed-use area, a relatively low-density residential area, and a purely expressway network connecting different satellite towns in the city. Due to the distinct land use patterns and geographical constraints, the transport networks were designed and built with different topological characteristics. Thus, the networks of the selected regions had different traffic capacities, offered drivers distinct free-flow travel speeds, and performed dissimilarly even under the same traffic loading.

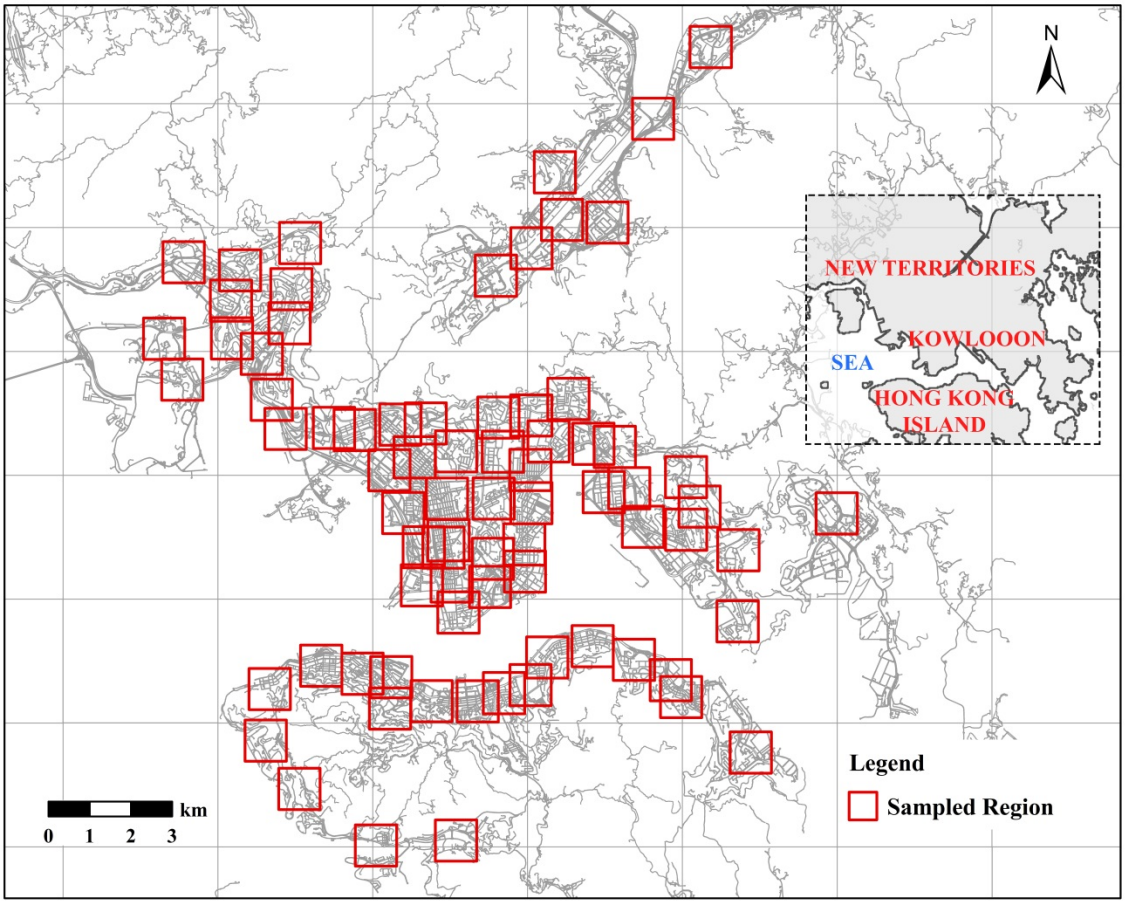

Figure 1. The Seventy one 1 km x 1 km regions of Hong Kong that were studied

3. Model calibration of the MBPR functions

The chosen MCF models of the 71 sampled regions must be calibrated to establish the relationship between the shape of the chosen MCF and the topological features of the network. The MBPR function, which is the chosen MCF model, is introduced in this section. The databases and the method of calculating the required data input for the model calibration are presented. The calibration results of the 71 studied regions are summarized.

3.1 MBPR function

The MBPR function, a polynomial type model depicting the network-wide travel time and traffic demand relationship, is defined as follows:

$$T = T_f + T_f \alpha Q^n, \tag{1}$$

where T is the travel time per unit of distance, measured in $\mathrm{h/km}$; T_f is the free-flow travel time, measured in $\mathrm{h/km}$; Q is the hourly total traffic flow entering the studied region, measured in $\mathrm{veh/h}$; α is the congestion sensitivity parameter, measured in $\mathrm{h^2/veh^2}$; and n is the model parameter. Note that in this case α absorbs the practical capacity of the network and thus differs from the usual definition of the dimensionless α in the link-based BPR function.

Model calibration for the MBPR function requires estimates of the hourly travel time per unit of distance and the hourly total traffic flow entering the studied region. The chosen candidate models were the MBPR functions with $n = 2, 3\ and\ 4$. In the free-flow state, the increase in travel time per unit of distance, ΔT, should be theoretically insensitive to an additional unit of traffic flow, ΔQ. Therefore, the first derivative of the travel time per unit of distance in relation to the hourly total traffic flow at zero flow should be zero. The linear model ($n = 1$), which did not satisfy this boundary condition, was therefore excluded from the pool of candidate models.

3.2 Database

The required traffic data for model calibration were obtained from data extracted from the 2010 taxi GPS database and the Annual Traffic Census (ATC) 2010 (Transport Department, 2010).

The taxi GPS database comprises detailed trip records of 480 GPS-equipped taxis from 2010. Each of the 480 probe vehicles reported their real-time location, expressed in WGS84 (the ITRF96 reference frame) in decimal degrees, and the date, time, traveling direction, instantaneous speed, and occupancy to the traffic control center every 30 seconds. Only the occupied taxis were taken into account in the model calibrations because they resembled the travel behavior of normal traffic. By plotting the data points of the taxis in a GIS software program, we traced the paths taken by each of the taxis. If the road network of

Hong Kong could be reproduced using the data points, the assumption that the probe taxis fully covered the area would be validated.

The ATC report provided detailed traffic data from over 1,500 stations covering approximately 90% of the trafficable roads in Hong Kong (Lam et al., 2003; Tong et al., 2003). The average annual daily traffic (AADT) across these ATC stations was obtained from the report.

3.3 Data constitutions

As the occupied taxis interacted with the other traffic around them when they travelled within the studied regions, all of the vehicles should have had similar speeds. Therefore, the arithmetic mean of the speeds of the occupied taxis within a studied region during a particular hour was taken as the unbiased estimate of the hourly space-mean speed of the traffic. The reciprocal of the hourly space-mean speed was the estimate of the hourly travel time per unit of distance, T.

The hourly total traffic flow entering a studied region, Q, was the sum of the hourly traffic flow entering the region via all of the links intercepting the boundary of a 1 km × 1 km network. However, as only a subset of the network links had been outfitted with on-road fixed detectors such as inductive loop detectors, it was impossible to directly and accurately measure the hourly total traffic flows across all of these links and hence the hourly total traffic flow was usually unobservable. Nevertheless, given the available taxi GPS database, the occupied taxi flows across all of the links, including the links intercepting the boundary of the selected network and the links within that network, were observable. The hourly total traffic flow can be alternatively expressed as the sum of the products of the hourly occupied taxi flow via a link intercepting the boundary and the total-traffic-to-occupied-taxi ratio, defined as a scaling factor hereafter, of the corresponding link. However, each of these scaling factors was unknown.

Given the geographical proximity of the roadways within each selected 1 km × 1 km network, the scaling factors of both the links intercepting the boundary and the links within that network were assumed to follow a distribution subject to a certain spatial variability, as it might have varied at different locations within the network due to various factors such as land use heterogeneity. As the ATC stations were outfitted with on-road fixed detectors and the AADT across the stations was observable, the stations within a studied region were chosen as the scaling factor sampling sites. The AADT of an ATC station divided by the average annual daily occupied taxi flow across the station was taken as the sampled scaling factor at that particular site. The average value of all of the sampled scaling factors was the expected total-traffic-to-occupied-taxi ratio of that network and estimated the mean of the scaling factor distribution. The variance of the sampled scaling factors measured the spatial variability of the scaling factor.

As the mean of the scaling factor distribution was the most likely observed traffic composition ratio of a studied region, the hourly total traffic flow entering that studied region was estimated by leveraging the linear data projection. Each hourly occupied taxi flow entering the studied region via a link intercepting the boundary was multiplied by the scaling factor mean instead of the corresponding unknown scaling factor. In other words, the sum of the products of the hourly occupied taxi flow via a link intercepting the boundary and the scaling factor mean (linearly projected data) estimated the hourly total traffic flow entering that studied region. The linearly projected hourly total traffic flows were then adjusted according to the ratio between the normalized traffic and occupied taxi flows hour by hour to account for the temporal effects before model calibration..

The MBPR function was then calibrated based on the constituted data. However, according to Wong and Wong (2015), model calibration based on linearly projected data can result in systematically biased calibrated parameters when the variability of the scaling factor, which may also contribute to the mean of the response variable, is ignored during calibration. Wong and Wong (2015) proposed the use of adjustment factors to capture the variability of the scaling factor and correct the systematically biased calibrated parameters. The proposed method was adopted in this paper to adjust the calibrated congestion sensitivity parameter of each studied region.

3.4 Calibration results

Regression analyses for the 71 sampled regions revealed that the MBPR function in quadratic form generally best represented the data. Compared with the model candidates with $n = 3$ and $n = 4$, the calibrated quadratic MBPR models best represented the collected data, giving the highest R-squared values and the lowest Akaike information criterion (AIC) values in 69 of the regions. The AIC provides the basis of comparison and selection among several models for a given set of data by measuring their relative quality in consideration of the trade-off between the goodness-of-fit and complexity of the model (Sakamoto et al., 1987). A model with the minimum AIC value is considered to be the most appropriate model. Only the West Kowloon and Choi Hung regions were best fitted by the cubic MBPR function, with slightly higher R-squared values and lower AIC values than the quadratic model. For West Kowloon, the R-squared values of the quadratic and cubic models were 0.478 and 0.515, respectively, and the AIC values of the quadratic and cubic models were -22957.0 and -23105.4, respectively. Similarly, for Choi Hung, the R-squared values of the quadratic and cubic models were 0.523 and 0.536, respectively, and the AIC values of the quadratic and cubic models were -24308.6 and -24365.4, respectively. As the cubic MBPR function only slightly better represented the data collected in two regions, whereas the cost-flow relationship of the vast majority of the sampled regions were best fitted by the quadratic MBPR model, the MBPR function with $n = 2$ was chosen as the MCF model for examining the network topology's effects on its model parameters: the free-flow travel time, T_f, and the congestion sensitivity parameter, α.

Two typical scatter plots with corrected best-fitting models from each of the major parts of Hong Kong—Hong Kong Island, Kowloon, and the New Territories—are presented in Figure 2. The scatter plots reveal that the travel time per unit of distance generally monotonically increased with increasing traffic demand. The increase in travel time per unit of distance was small when the traffic demand was small. However, the travel time increased dramatically as the traffic loading exceeded the network practical capacity, demonstrating the effect of congestion in a network. The fitted curves follow the trends of the scatter plots and lie well within the scattered data points, indicating satisfactory fitting. The free-flow travel time and the curvature of each of the fitted curves in Figure 2 differ due to the topological differences in the sampled networks.

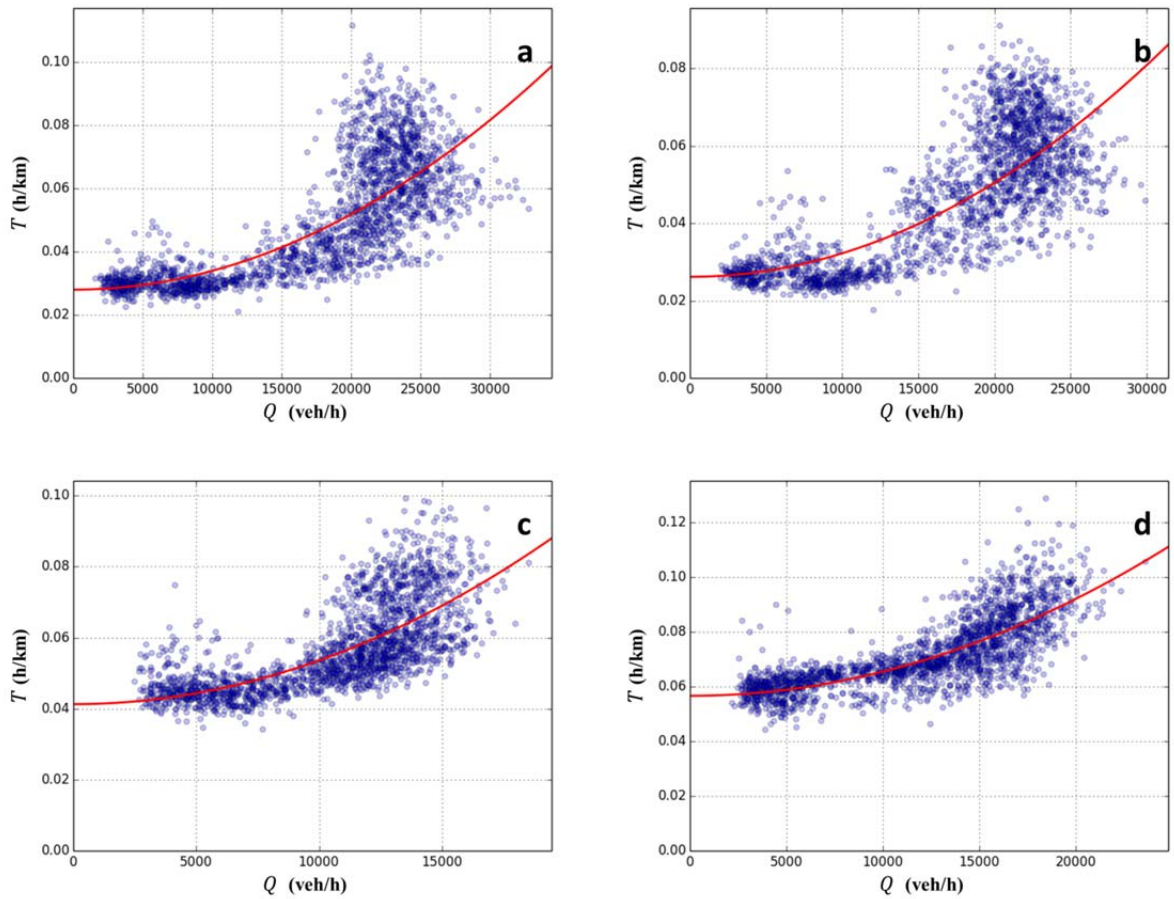

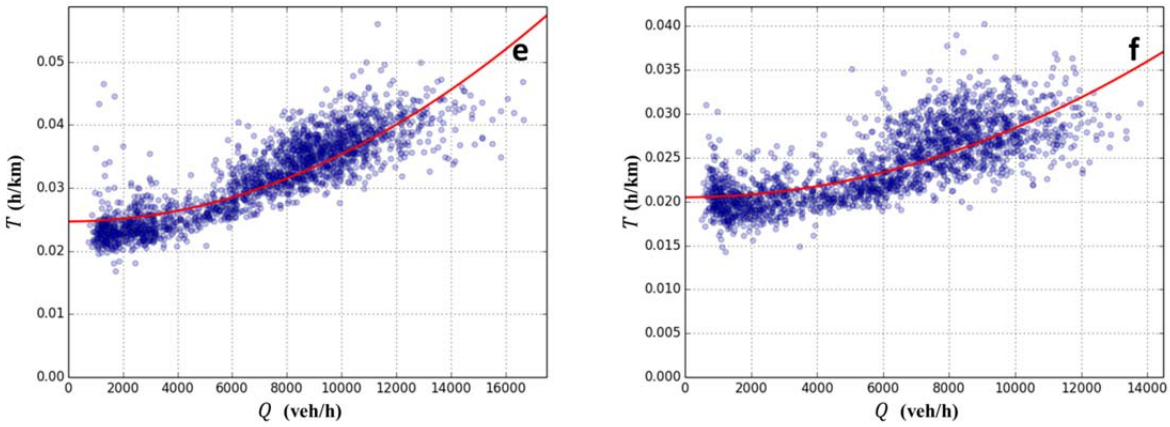

Figure 2. Scatter plots and best-fitting MBPR functions of representative regions: (a) Wan Chai in Hong Kong Island, (b) Causeway Bay in Hong Kong Island, (c) Mong Kok in Kowloon, (d) Prince Edward in Kowloon, (e) Lai King in the New Territories, and (f) Kwai Chung Park in the New Territories.

Table 1 shows the range, means, and standard deviations of the calibrated free-flow travel time, T_f, and the adjusted congestion sensitivity parameter, α, for the 71 fitted quadratic MBPR functions. The resultant free-flow speeds, u_f, are also presented in Table 1.

Table 1. Summary of the calibrated parameters

Parameter / Metric	Minimum	Maximum	Mean	S. D.
T_f (h/km)	0.0133	0.0624	0.0313	0.0107
u_f (km/h)	16.03	74.97	35.70	12.12
α (h^2/veh^2)	9.058E-10	1.921E-8	4.261E-9	3.811E-9

The free-flow travel time, T_f, and congestion sensitivity parameter, α, are the parameters governing the shape of the chosen MBPR function. They varied across the 71 sampled regions. Network topologies influenced the driving behavior of road users and hence the performance of the transport network. The shape of the chosen MBPR function and the governing parameters (i.e., T_f and α) were therefore closely related to the topological features of the network. In other words, the calibrated MBPR functions of the 71 sampled regions with different combinations of T_f and α resulted from their own topological features.

4. Network topological effects on the parameters of the MBPR function

Apart from the parameters of the MBPR functions calibrated in the previous section, a set of metrics capturing the topological features of each of the 71 sampled regions were essential ingredients in our investigation of the relationship between the shape of the chosen MBPR function and the topological features of the network.

Macroscopic models are the essential inputs of continuum modeling for urban cities. The continuum modeling approach is usually adopted when detailed information about the

transportation system and traffic data are unavailable and the focus is on the general trend and pattern of traffic flow or the changes in that traffic flow resulting from policy changes in the transportation system at the macroscopic rather than detailed level. Assuming the unavailability of detailed network and traffic information, we selected and formulated topological metrics that were readily obtainable from maps via certain image-processing procedures. These topological metrics that may play a critical role in affecting the shape of the MBPR were introduced and calculated in this section. The pertinent topological data were extracted using GIS software. Then the free-flow travel time and congestion sensitivity parameter related to these topological metrics was comprehensively studied to develop the SVMBPR function.

4.1. Potential topological metrics influencing the free-flow travel time

During very light traffic demand, vehicles can travel freely on a road network without interacting with other road users and without delay due to congestion. The time required for them to travel a unit of distance is the free-flow travel time of the network. In these cases, it is obvious that junctions are the major causes of travel delays. Junctions are the intersections in the road network at which traffic streams conflict with each other. They can be classified as signalized junctions, priority junctions, or roundabouts. For safety, drivers have to stop when they encounter a red signal traffic light or slow down as they approach a priority junction or a roundabout. The network free-flow travel time is deemed to decrease with the junction density of the network. We defined three types of junction densities and examined their relationship with the free-flow travel time. Moreover, links are connected at junctions. Therefore, a network with greater junction density normally implies a well-connected network. In other words, junction density can be considered as a proxy measure of connectivity.

The first junction density, γ_g, was defined as the total number of junctions divided by the gross area of the sampled region, A_g. The gross area is the sum of both the trafficable area, A_t, and non-trafficable area, A_n, within the region (i.e., $A_g = A_t + A_n$). Trafficable area was defined as the road space area. As all 71 sampled regions were standard square boxes with areas of square kilometer, this metric was equivalent to the total number of junctions within each studied region. Junctions are the primary causes of travel delay. A longer free-flow travel time was expected if there were more junctions in a sampled region.

The total number of junctions per unit trafficable area, γ_t, was defined as the second junction density measure. It was suspected that the total number of junctions correlated with the trafficable area because a larger trafficable area normally implies more junctions within the network, to maintain an acceptable level of accessibility and route choice combinations. The non-trafficable area within a selected region does not facilitate the movement of traffic and hence has no effect on the network free-flow travel time. Normalizing the junction density using the trafficable area may provide not only a more relevant metric, but also a more comparable metric because the trafficable areas of the sampled regions differed.

The last junction density, γ_d, was the average number of junctions per unit of distance, or the reciprocal of the average junction spacing (i.e., $\gamma_d = 1/\bar{s}$). The average junction spacing of a sampled region, $\bar{s}$, was obtained by taking the mean of the length of all links associated with that studied region. The length of a link is the distance between its upstream and downstream junctions. The width of a link normally indicates the number of lanes of a roadway. It may provide vehicles with opportunities to overtake vehicles ahead of them by changing lanes, but it was anticipated to have minimal effects on the free-flow travel time during the free-flow state. This metric, which only takes the lengths of the links into consideration, further filters the information about the width of the road from the trafficable area. More junctions per unit kilometer of road result in more stop-and-go motions and more travel delay. Road users are therefore forced to travel for a longer free-flow travel time on average during free-flow. The free-flow travel time was predicted to be positively correlated with the average number of junctions per unit of distance. Moreover, we anticipate that junction spacing is highly correlated with both road hierarchies and speed limits. Freeways and expressways allow drivers to travel at high speeds and are characterized by larger junction spacing, whereas local urban links impose lower speed limits and are characterized by shorter junction spacing. Thus, this junction density can be considered as a proxy measure for the speed limit and road hierarchy of a link.

4.2. Potential topological metrics influencing the congestion sensitivity parameter

The congestion sensitivity parameter measures how easily congestion develops within a studied region when traffic demand increases. It plays a key role in increasing travel time in relation to a unit increase in traffic loading. The number of alternative routes available to road users and the capacity of the network are thought to be the primary factors determining the congestion sensitivity parameter. Road density, the first junction density defined in the previous sub-section, the total number of links, and the total length of the links, were expected to be the metrics correlated with the congestion sensitivity parameter.

We defined road density, ρ, as the percentage of trafficable area within the total sampled area. It was calculated by dividing the total trafficable area by the gross sampled area (i.e., $\rho = A_t/A_g \times 100\%$). It captured information about the total length and the number of lanes of links within a sampled region. As the road capacity of a network should be positively correlated with the total length and widths of links, this metric can be considered as a proxy measure for road capacity. A higher road density leads to a higher capacity and higher jam density, as more road space is available to serve more road users and more vehicles can be packed onto the road network when serious traffic congestion occurs. In the dense urban network context, traffic links are usually well connected at junctions to ensure high accessibility. Thus, the trafficable area of a network generally increases with the number of junctions. As junctions provide opportunities for rerouting, a larger number of junctions means more route choices. In such cases, a greater trafficable area implies more route choices. If the road density of a sampled region is high, then drivers are more likely to be able to reroute their vehicles to prevent themselves from being stranded when they encounter a

serious traffic jam. Thus, road density captures information about both the capacity of the network and the available route choices. This metric was expected to be negatively correlated with the congestion sensitivity parameter.

Junctions provide opportunities for road users to change direction and reroute their vehicles when there is traffic congestion. The first junction density, γ_g, defined in the previous sub-section, was thus a measure of the available route choices. A large number of junctions implies more available alternative routes and decreases the chance of being stranded during congestion. The congestion sensitivity parameter was therefore expected to decrease with this metric.

The total number of links per unit area, τ, was another topological metric expected to be correlated with the congestion sensitivity parameter. The total number of links was expected to be correlated with the number of junctions within the sampled region because links join each other at junctions. This metric was therefore also a measure of the available alternative route choices. More roads generally offer drivers more route choice combinations. Similarly, drivers can easily avoid getting into a traffic jam by taking an alternative path if more alternative route choices exist. In other words, the cost flow function becomes less sensitive toward increases in traffic demand. A decreasing trend between the total number of links and the congestion sensitivity parameter was anticipated.

The last metric was the total length of links, denoted by L. This topological metric, similar to road density, captured information about both the network capacity and the available route choices in the selected network. However, it ignored the widths of the road segments. With a larger total length of links, a greater network capacity and more route choices were expected. A negative correlation between the congestion sensitivity parameter and the total length of links was therefore expected.

4.3. Extraction of the topological data

Elementary topological data, such as the trafficable area of each sampled region, the numbers of junctions and links, and the length of each link associated with these regions, were first collected using GIS software. The proposed topological metrics discussed in the previous two sub-sections were then calculated.

As an illustrative example, Prince Edward in Kowloon (shown in Figure 3) is used to demonstrate how the topological data were extracted. The free-flow travel time and corrected congestion sensitivity parameter of Prince Edward were calibrated and adjusted to be 0.0566 h/km and 1.564 $\mathrm{h}^2/\mathrm{veh}^2$, respectively. Prince Edward is characterized by a grid of urban streets and roads. It is a highly dense commercial and residential mixed use area in Hong Kong. The shaded grey areas in Figure 3 are the non-trafficable areas, A_n, and the unshaded areas are the trafficable areas, A_t. The total trafficable area enclosed by the square box was evaluated using GIS software. The road density of Prince Edward was 26.5%, indicating that the trafficable area was slightly more than one fourth of the sampled area.

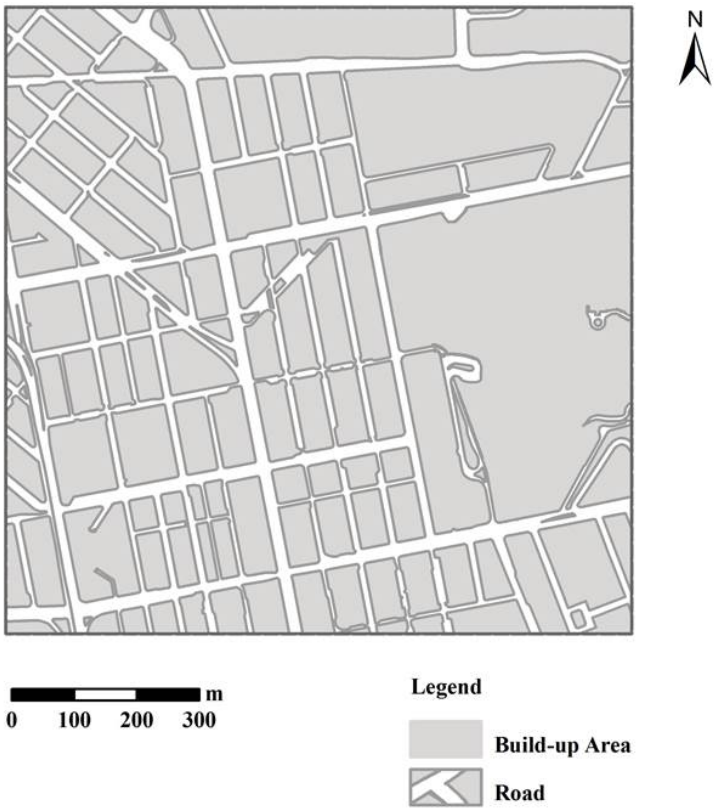

Figure 3. Map of Prince Edward in Kowloon

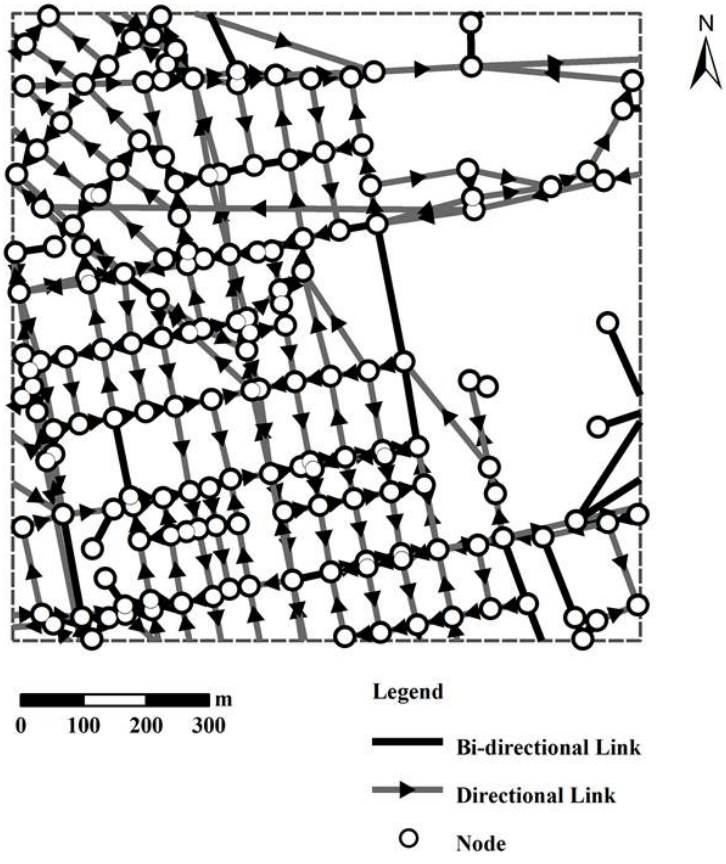

Figure 4. Primal representation of Prince Edward in Kowloon

The primal approach was used to transform the planar road network of Prince Edward into the node-link form shown in Figure 4. The primal presentation, which represents road segments as links and junctions as nodes, is an intuitive, natural approach (Crucitti et al., 2006; Cardillo et al., 2006; Porta et al., 2006). This representation preserves the geometric patterns and geographical properties of the transportation network (Lin and Ban, 2013). In Figure 4, junctions at which traffic streams conflict are represented by circular nodes. The thicker dark lines represent bi-directional links and the lines with arrows represent directional links.

The first two junction densities and the total number of links associated with the studied region were evaluated by counting the number of junctions and links. In this example, $\gamma_g = 172$ junctions/km^2 , $\gamma_t = 649.8$ junctions/km^2 and $\tau = 360$ links/km^2 . For simplicity, road segments were transformed into straight lines joining the upstream and downstream junctions. The length of each link was calculated with GIS software. The remaining topological metrics, including the total length of links ($L = 34.2$ km) and average number of junctions per kilometer ($\gamma_d = 10.5$ junctions/km), were also calculated.

The above procedures were repeated for each of the 71 regions, giving the required potential topological data. Table 2 summarizes the collected data, including the ranges, mean values, and standard deviations. The effects of these topological metrics on the calibrated free-flow travel time and corrected congestion sensitivity parameter were then studied to obtain the best-fitting mathematical models.

Table 2. Summary of the collected topological data

Parameter / Metric	Minimum	Maximum	Mean	S. D.
γ_g(junction/km^2)	27	179	89	35.4
γ_t (junction/km^2)	201.0	702.7	469.7	119.2
γ_d (junction/km)	3.353	10.995	7.017	1.715
ρ (%)	9.958	29.501	18.695	4.610
τ (links/km^2)	67	360	193.8	67.3
L (km)	14.252	43.077	27.068	6.813

4.4. Effects of topological features on the free-flow travel time

This subsection presents comprehensive regression analysis of the effects of the three topological metrics proposed in Section 4.1 on the free-flow travel time of the 71 MBPR functions calibrated in Section 3. Table 3 presents the results of the regression analysis.

Table 3. Effects of topological features on the free-flow travel time

Topological Metric	Model Form	R-square	AIC
γ_g	$T_f = a\gamma_g + b$	0.122	-647.4
	$T_f = a{\gamma_g}^2 + b$	0.120	-647.3
	$T_f = a{\gamma_g}^3 + b$	0.114	-646.8
	$T_f = a\ exp(b\gamma_g)$	0.123	-647.5
γ_t	$T_f = a\gamma_t + b$	0.332	-666.8
	$T_f = a{\gamma_t}^2 + b$	0.327	-666.3
	$T_f = a{\gamma_t}^3 + b$	0.313	-664.9
	$T_f = a\ exp(b\gamma_t)$	0.331	-666.7
γ_d	$T_f = a\gamma_d + b$	0.434	-678.6
	$T_f = a{\gamma_d}^2 + b$	0.434	-678.6
	$T_f = a{\gamma_d}^3 + b$	0.424	-677.4
	$T_f = a\ exp(b\gamma_d)$	0.437	-679.0

A greater number of junctions within a network normally implies a longer travel time at the free-flow state. However, the poor regression results with low R-square values of around 0.12 and high AIC values of around -647 based on γ_g suggested that γ_g failed to act as the explanatory factor accounting for the variation of free-flow travel time among the 71 sampled regions. γ_g failed to capture information about the spatial distribution of the junctions within a sampled network. For instance, if there is a sampled network with a certain value of γ_g and the junctions within the network are closely spaced, then a vehicle traveling through this network must experience more frequent stop-and-go motions than it would traveling through a sampled network with the same value of γ_g and widely spaced junctions. Therefore, it is difficult for a vehicle traveling through a network with closely spaced junctions to attain a high speed and complete the trip with a shorter travel time, even in the free-flow state. As the spatial distribution of junctions plays a critical role in governing the free-flow travel time of a network and γ_g failed to capture such an important factor, regression analyses resulted in very low R-square and high AIC values. However, after replacing γ_g with γ_t, the R-square and AIC values of the calibrated models increased to around 0.32 and dropped to around -666, respectively. This confirmed that normalizing the total number of junctions within a sampled region by its trafficable area and removing the non-trafficable area from the denominator indeed formulated and provided a better and more relevant topological metric accounting for the variation of free-flow travel time among the sampled networks. In addition to further filtering the information about the width of links from the trafficable area, γ_d represented the average spatial distribution of the junctions, as the average junction spacing was a point estimator of the linear spatial distribution of the

junctions. The improved regression results with R-square values of around 0.43 and AIC values of around -678 based on γ_d provided evidence that γ_d rather than simply the total number of junctions within a sampled network was the primary factor governing the free-flow travel time of a network.

The best-fitting exponential function relating the free-flow travel time and average number of junctions per kilometer, with the highest R-square value (0.437) and lowest AIC value (-679.0), was selected:

$$T_f = a\ exp[b\gamma_d(x,y)], \tag{2}$$

where $\gamma_d(x,y)$ is the average number of junctions per kilometer round the vicinity (1 km $\times$ 1 km network) of the point (x,y), measured in $\mathrm{junction/km}$; a is the free-flow travel time with 0 junctions per kilometer on average; and b is the number of times the free-flow travel time grows by a factor e per unit increase in the average number of junctions per kilometer.

The scatter plot of the calibrated free-flow travel time against the average number of junctions per kilometer and the best-fitting exponential model are shown in Figure 5. The calibrated a was $0.0124\ \mathrm{h/km}$, with 95% confidence intervals for the lower and upper bounds of $0.0090\ \mathrm{h/km}$ and $0.0158\ \mathrm{h/km}$, respectively. The calibrated b was $0.128\ \mathrm{km/junctions}$, with 95% confidence intervals for the lower and upper bounds of $0.094\ \mathrm{km/junctions}$ and $0.163\ \mathrm{km/junctions}$, respectively. The free-flow travel time increased exponentially with the average number of junctions per unit kilometer. The strictly increasing relationship was consistent with our expectations. For each unit increase in the average number of junctions per kilometer, the free-flow travel time increased by a factor of $e^{0.128}$. The free-flow travel time in a region with 0 junctions per kilometer on average was $0.0124\ \mathrm{h/km}$. By taking the reciprocal of the calibrated value of a, the free-flow speed of a 1 km x 1 km region with road segments with no junctions on average was calculated to be 80.5 km/h, which was consistent with our real-life experience.

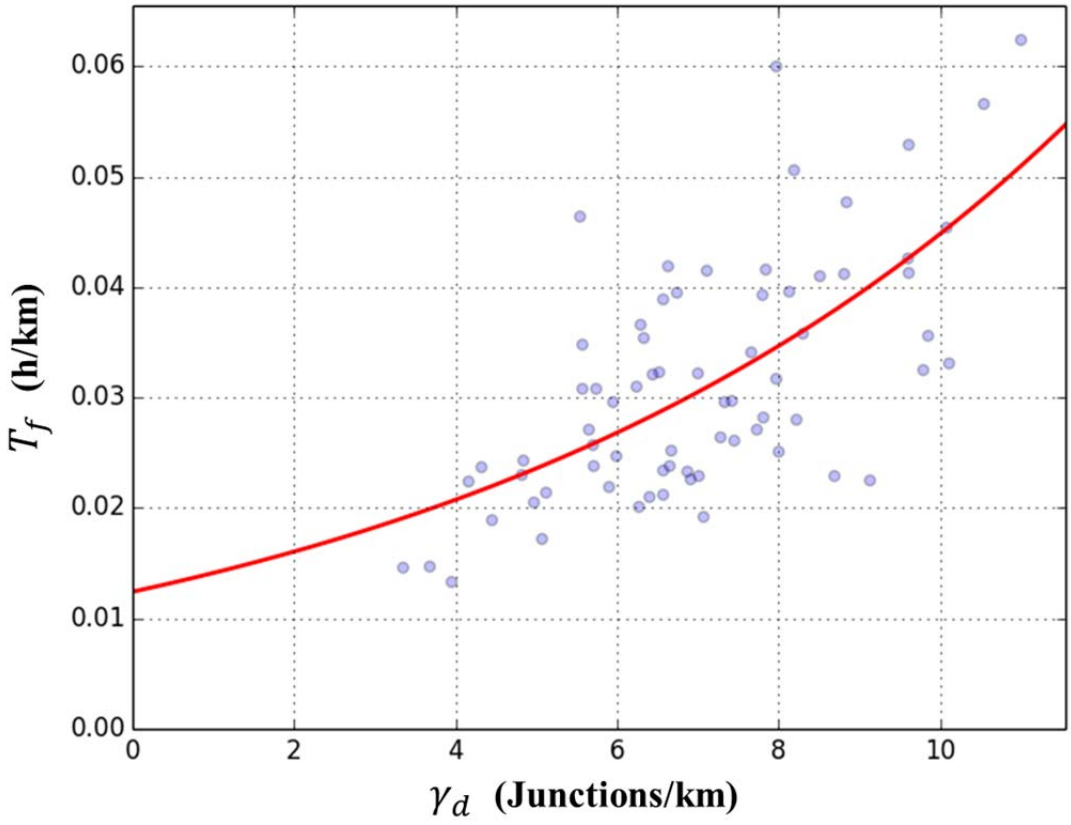

Figure 5. Scatter plot of the calibrated free-flow travel time against the average number of junctions per unit kilometer and the best-fitting model (R-square = 0.437, AIC = -679.0).

4.5. Effects of topological features on the congestion sensitivity parameter

Various model forms were selected for the regression analysis of the corrected congestion sensitivity parameters of the 71 sampled regions and the collected topological data to study how the four proposed topological metrics influenced the congestion sensitivity parameter. Table 4 summarizes the results.

The road density was the major factor in determining the value of the congestion sensitivity parameter of the sampled networks. The best-fitting model relating the congestion sensitivity parameter and road density, with the highest R-square value (0.561) and lowest AIC value (-2805.2), was chosen:

$$\alpha = \frac{c}{\rho(x,y) - d}, \tag{3}$$

where $\rho(x,y)$ is the road density round the vicinity (1 km × 1 km network) of the point (x,y), measured in %; and c and d are the model parameters.

Table 4. Effects of topological features on the congestion sensitivity parameter

Topological Metric	Model Form	R-square	AIC
ρ	$\alpha = c/\rho$	0.320	-2776.1
	$\alpha = c/(\rho - d)$	0.561	-2805.2
	$\alpha = c\rho^d$	0.531	-2800.5
	$\alpha = exp(-\rho - c)/(\rho - d)$	0.559	-2804.9
γ_g	$\alpha = c/\gamma_g$	0.263	-2770.4
	$\alpha = c/(\gamma_g - d)$	0.263	-2768.4
	$\alpha = c{\gamma_g}^d$	0.263	-2768.4
	$\alpha = exp(-\gamma_g - c)/(\gamma_g - d)$	0.263	-2768.4
τ	$\alpha = c/\tau$	0.255	-2769.6
	$\alpha = c/(\tau - d)$	0.256	-2767.7
	$\alpha = c\tau^d$	0.258	-2767.9
	$\alpha = exp(-\tau - c)/(\tau - d)$	0.261	-2768.2
L	$\alpha = c/L$	0.281	-2772.1
	$\alpha = c/(L - d)$	0.373	-2779.9
	$\alpha = cL^d$	0.401	-2783.1
	$\alpha = exp(-L - c)/(L - d)$	0.374	-2780.0

The scatter plot of the corrected congestion sensitivity parameter against the road density and the best-fitting model are shown in Figure 6. The calibrated c was 3.438×10^{-10} h^2/veh^2, with 95% confidence intervals for the lower and upper bounds of 2.643×10^{-10} h^2/veh^2 and 4.233×10^{-10} h^2/veh^2, respectively. The calibrated d was 8.096%, with 95% confidence intervals for the lower and upper bounds of 7.372% and 8.820%, respectively. The congestion sensitivity parameter, which here measured how easily traffic congestion developed within a one kilometer square road network, generally decreased with the road density. The correlation between γ_g and ρ of the 71 sampled networks was 0.736. This high correlation implied that the number of junctions within a network generally increased with the network's road density. Therefore, in the dense urban network context, an increase in road density generally means an increase in network capacity and an increase in the number of alternative routes. These all help to reduce the sensitivity of the travel time toward the increase in network traffic demand.

The congestion sensitivity parameter dropped dramatically as the road density increased when the road density was below approximately 15%. A small increase in the road

density therefore effectively provided alternative route choices for drivers to reroute their vehicles and avoid traffic jams.

However, the rate of the decrease in congestion sensitivity diminished gradually as the road density exceeded about 15%. The diminishing effect of the reduction in congestion sensitivity showed that further increases in road density were ineffective at decreasing the sensitivity of the travel time toward increases in traffic demand. This could have been a result of both the random delay effect caused by the increased number of junctions and user equilibrium. The high correlation between ρ and γ_g (0.736) provided evidence that the number of junctions within a selected network generally increased with the network's road density. As the number of junctions increased, the random delay effect accumulated and counteracted the contribution of additional road space to decreasing the congestion sensitivity parameter. As the road density exceeded about 15%, the random delay effect caused by the additional number of junctions might have been be comparable with the contribution of additional road space. Thus, these effects gradually balanced each other out and the congestion parameter was gradually stabilized. In addition to the random delay effect, a further increase in road density might not have always contributed to lowering the congestion sensitivity parameter. Under user equilibrium, road users always choose the shortest path with the lowest travel cost. Therefore, if the additional road segments were not able to divert traffic to its desired destinations or if the travel costs involved in taking these additional paths were equal to or greater than the cost of the congested path, then an increase in road density might have been ineffective in addressing and easing the traffic congestion.

It is worth noting that the calibrated vertical asymptote was situated at $\rho = 8.096\%$, or the suggested minimum road density for macroscopic models. This implies that macroscopic models are only applicable to relatively dense urban networks with road densities greater than 8.096%. On the contrary, if the road density of a network is very low, i.e., less than 8.096%, then the network capacity is low and there may be fewer available route choices. In such cases, the transportation network is prone to traffic congestion even with a small increase in traffic demand. This kind of network is no longer considered as a dense network and should be modeled using the discrete modeling approach instead of the continuum modeling approach. Based on the collected data, we interpret the calibrated vertical asymptote as the minimum road density using the continuum modeling approach. For some networks involving both high-density ($\rho > 8.096\%$) and low-density ($\rho < 8.096\%$) road networks, such as satellite towns connected by freeways or bridges, a hybrid modeling approach (Yang et al., 1994; Wong et al., 2003), which is an integrated or combined approach involving both the discrete and the continuum modeling approaches, should be adopted.

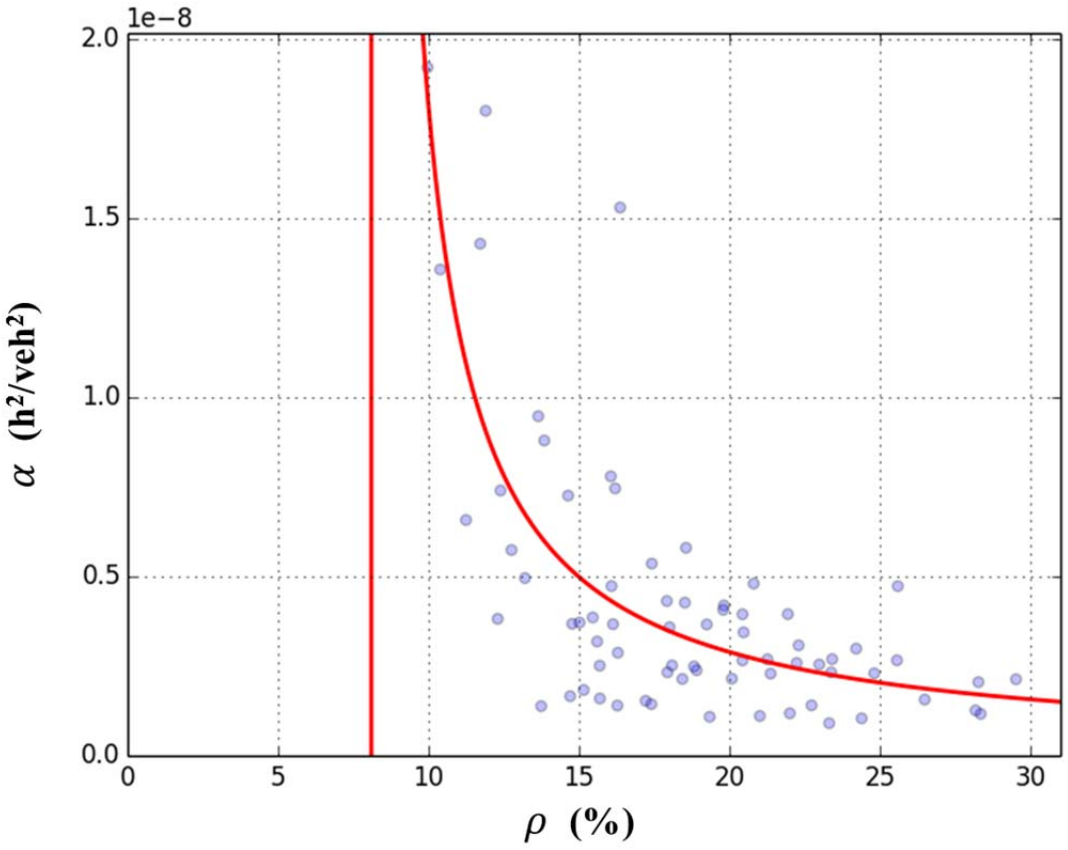

Figure 6. Scatter plot of the corrected congestion sensitivity parameter against road density and the best-fitting model (R-square = 0.561, AIC = -2805.2).

4.6. SVMBPR function

The average number of junctions per unit of distance and the road density were found to be the topological metrics that best correlated with the free-flow travel time and the congestion sensitivity parameter, respectively. As these topological metrics varied spatially, the SVMBPR was established by directly substituting the spatially variable free-flow travel time and the spatially variable congestion sensitivity parameter into the MBPR function. The developed SVMBPR function is as follows:

$$T = 0.0124\ exp[0.128\gamma_d(x,y)]\left[1 + \frac{3.438 \times 10^{-10}}{\rho(x,y) - 8.096\%}Q^2\right]. \quad (4)$$

The SVMBPR function extends the average travel time within a network from a function solely dependent on the hourly total traffic demand Q to a function dependent on both the spatially variable network topological characteristics and the traffic demand. The average travel time required for traveling a unit of distance within the network increased with the number of junctions per unit distance, γ_d. The increase in travel time was less sensitive to the increase in traffic demand as the road density of the network ρ increased. The developed

SVMBPR function is only applicable to a dense urban network with a road density greater than 8.096%, which is the suggested minimum road density for macroscopic models.

The developed SVMBPR function offers a good estimation of the MBPR function of a network by inputting the average number of junctions per unit kilometer and the road density of the network. Compared with traffic data collected across a wide network over several years, these topological data can be readily acquired from maps using image processing. In developing countries, traffic data collected from advanced wireless devices may not always be feasible. MCFs are therefore important and helpful for initial land use planning during rapid urbanization.

Moreover, we adopted a two-stage model calibration procedure rather than an integrated model calibration procedure in this study to calibrate the functional expressions for the spatially variable free-flow travel time and the spatially variable congestion sensitivity parameter. As the SVMBPR function is a nonlinear function of the linearly projected hourly total traffic flow, an integrated model calibration procedure based on the linearly projected data ignored the effects of variability of the scaling factors and led to systematically biased calibrated parameters (see Wong and Wong, 2015). Future research could develop an integrated model calibration procedure to further improve the accuracy of the SVMBPR function parameter estimations.

5. Conclusion

The topological features of a network directly affect its performance at different levels of traffic demand. For the sake of developing a more efficient transport system, it is therefore important to understand how the network topologies and the shape of the MCF of the corresponding network correlate with each other. This paper reveals the relationship between junction density, γ_d, defined as the reciprocal of the average junction spacing, and the free-flow travel time within a network, T_f, and the relationship between the road density, ρ, and the congestion sensitivity parameter, α. It uses these relationships to develop the SVMBPR function.

Seventy one 1 km × 1 km real-world networks with dissimilar topological features were sampled from Hong Kong, which is one of the most highly urbanized cities with a dense network in the world. The MBPR functions for the selected regions were calibrated based on a combination of a year of taxi GPS data and traffic data extracted from the ATC. We proposed seven topological metrics that potentially correlated with the model parameters of the MBPR function. The elementary topological data were extracted using GIS software and were integrated to obtain the seven proposed metrics for each of the sampled regions. Intensive investigation revealed that the free-flow travel time within a network increased exponentially with the average number of junctions per unit of distance. The congestion sensitivity parameter of a network dropped sharply as the road density increased from 8.096% to around 15.0%. The decrease in the congestion sensitivity parameter due to further

increases in road density was minimal once it exceeded 15.0%. A road density of 8.096% is suggested as the minimum road density for macroscopic models. The established direct relationships between the topological metrics and the model parameters of the MBPR function provide us with a better understanding of the influence of a network's topology on its performance. This is helpful for planners and engineers during initial network design.

The developed SVMBPR function expresses the average travel time per unit of distance as a function of both the traffic demand and the spatially variable network topological metrics. This function can easily provide a good approximation of the MBPR function of a network using only the corresponding road density and average number of junctions per unit distance. These topological data are more readily available and relatively cheaper to collect than traffic data.

Although the SVMBPR function was developed based on the traffic data in Hong Kong, the proposed methodology is not localized and can in principle be directly transferred to other dense urban networks. However, to ascertain this transferability, the calibrated parameters of the SVMBPR function must be validated using GPS data from other cities before the methodology can be universally applied. This presents an interesting direction for future work.

Moreover, the developed SVMBPR model does not account for the origin-destination patterns. However, origin-destination-specific models might perform better in policy analysis. Thus, the development of origin-destination specific models offers a possible future research direction. MFDs, which model the average vehicular speed, flow and vehicular density over a network-wide region, comprise a class of models that depict macroscopic traffic dynamics. Daganzo (2007) recently proposed that MFDs were a property of a network infrastructure only while the infrastructure was independent of traffic demand. In a field study, Geroliminis and Daganzo (2008) confirmed that MFDs existed and were independent of origin-destination tables. This has aroused considerable interest in the topic of MFDs such as MFDs for inhomogeneous networks (Xie et al., 2015) and the potential applications of MFDs in network-wide traffic management and control (see Gayah, Gao and Nagle, 2014; Leclercq, Chiabaut and Trinquier, 2014; Aboudolas and Geroliminis, 2013; Geroliminis, Haddad and Ramezani, 2013; Ortigosa, Menendez and Tapia, 2013). Although the existence of MFDs has been verified using empirical data, the estimation of such a relationship remains notably difficult in practice (Nagle and Gayah, 2014). Exploration of the topological effects of a network on the shape of an MFD and the development of a spatial variable MFD might provide an easier and simpler means of estimating the MFD of a network.

Acknowledgements

The work presented in this paper was supported by a Research Postgraduate Studentship and grants from the Research Grants Council of the Hong Kong Special Administrative Region, China (Project No. 17208614). We would like to express our sincere gratitude to Concord Pacific Satellite Technologies Limited and Motion Power Media Limited for the provision of

the taxi GPS data and the Transport Department of the HKSAR government for the traffic flow data from the ATC used in this research work.

References

Aboudolas, K., Geroliminis, N., 2013. Perimeter and boundary flow control in multi-reservoir heterogeneous networks. *Transportation Research Part B: Methodological,* 55, 265-281.

Akçelik, R., 1978. A new look at Davidson's travel time function. *Traffic Engineering & Control,* 19**,** 459-463.

Akçelik, R., 1981. *Traffic signals: capacity and timing analysis,* Research Report 123, Australian Road Research Board, Melbourne, Australia.

Akçelik, R., 1991. Travel time functions for transport planning purposes: Davidson's function, its time dependent form and alternative travel time function. *Australian Road Research,* 21**,** 44-59.

Branston, D., 1976. Link capacity functions: A review. *Transportation Research,* 10**,** 223-236.

Bureau of Public Roads, 1964. Traffic Assignment Manual. *US Department of Commerce, Urban Planning Division, Washington DC.*

Cardillo, A., Scellato, S., Latora, V., Porta, S., 2006. Structural properties of planar graphs of urban street patterns. *Physical Review E,* 73**,** 066107.

Cetin, M., Foytik, P., Son, S., Khattak, A.J., Robinson, R. M., Lee, J., 2012. Calibration of volume-delay functions for traffic assignment in travel demand models. Paper presented at *the 91st Annual Meeting of Transportation Research Board.* Washington DC.

Crucitti, P., Latora, V., Porta, S., 2006. Centrality measures in spatial networks of urban streets. *Physical Review E,* 73**,** 036125.

Daganzo, C.F., 2007. Urban gridlock: Macroscopic modeling and mitigation approaches. *Transportation Research Part B: Methodological,* 41**,** 49-62.

Davidson, K.B., 1966. A flow travel time relationship for use in transportation planning. Australian Road Research Board (ARRB) Conference, 3rd, Sydney, 183-194.

Davidson, K.B., 1978. The theoretical basis of a flow-travel time relationship for use in transportation planning. *Australian Road Research,* 8**,** 32-35.

Davis, G.A., Xiong, H., 2007. *Access to destinations: travel time estimation on arterials.* Minnesota: Minnesota Department of Transportation, Office of Research Services.

Dowling, R.G., Singh, R., Cheng, W.W.K., 1998. Accuracy and performance of improved speed-flow curves. *Transportation Research Record: Journal of the Transportation Research Board,* 1646**,** 9-17.

García-Ródenas, R., Verastegui-Rayo, D., 2013. Adjustment of the link travel-time functions in traffic equilibrium assignment models. *Transportmetrica A: Transport Science,* 9**,** 798-824.

Gayah, V.V., Gao, X.S.,, Nagle, A.S., 2014. On the impacts of locally adaptive signal control on urban network stability and the macroscopic fundamental diagram. *Transportation Research Part B: Methodological,* 70, 255-268.

Geroliminis, N., Daganzo, C.F., 2008. Existence of urban-scale macroscopic fundamental diagrams: Some experimental findings. *Transportation Research Part B: Methodological,* 42**,** 759-770.

Geroliminis, N., Haddad, J., Ramezani, M., 2013. Optimal perimeter control for two urban regions with macroscopic fundamenal diagrams: a model predictive approach. *IEEE Transactions on Intelligent Transportation System,* 14 (1), 348-359.

Golding, S., 1977. On Davidson's flow/travel time relationship. *Australian Road Research,* 7**,** 36-37.

Ho, H.W., Wong, S.C., 2006. Two-dimensional continuum modeling approach to transportation problems. *Journal of Transportation Systems Engineering and Information Technology,* 6**,** 53-68.

Ho, H.W., Wong, S.C., 2007. Housing allocation problem in a continuum transportation system. *Transportmetrica,* 3**,** 21-39.

Ho, H.W., Wong, S.C., Hau, T.D., 2007. Existence and uniqueness of a solution for the multi-class user equilibrium problem in a continuum transportation system. *Transportmetrica,* 3**,** 107-117.

Ho, H.W., Wong, S.C., Loo, B.P.Y., 2004. Sequential optimization approach for the multi-class user equilibrium problem in a continuous transportation system. *Journal of advanced transportation,* 38**,** 323-345.

Ho, H.W., Wong, S.C., Yang, H., Loo, B.P.Y., 2005. Cordon-based congestion pricing in a continuum traffic equilibrium system. *Transportation Research Part A: Policy and Practice,* 39**,** 813-834.

Ho, H.W., Wong, S.C., Loo, B.P.Y., 2006. Combined distribution and assignment model for a continuum traffic equilibrium problem with multiple user classes. *Transportation Research Part B: Methodological,* 40**,** 633-650.

Ho, H.W., Sumalee, A., Lam, W.H.K., Szeto, W.Y. 2013a. A Continuum Modeling Approach for Network Vulnerability Analysis at Regional Scale. *Procedia-Social and Behavioral Sciences,* 80**,** 846-859.

Ho, H.W., Wong, S.C., Sumalee, A. 2013b. A congestion-pricing problem with a polycentric region and multi-class users: a continuum modelling approach. *Transportmetrica A: Transport Science,* 9**,** 514-545.

Huntsinger, L.F., Rouphail, N.M., 2011. Calibrating travel demand model volume-delay functions using bottleneck and queuing analysis. Paper presented at *the 90th Annual Meeting of the Transportation Research Board.* Washington, DC.

Jastrzebski, W., 2000. Volume delay functions. 15th International EMME/2 Users Group Conference, Vancouver, BC.

Klieman, L., Zhang, W., Bernardin JR, V. L., Livshits, V., 2011. Estimation and comparison of volume delay functions for arterials and freeway HOV and general purpose lanes. Paper presented at *the 90th Annual Meeting of Transportation Research Board.* Washington DC.

Lam, W.H.K., Hung, W.T., Lo, H.K., Lo, H.P., Tong, C.O., Wong, S.C., Yang, H., 2003. Advancement of the annual traffic census in Hong Kong. *Proceedings of the ICE-Transport,* 156**,** 103-115.

Leclercq, L., Chiabaut, N., Trinquier, B., 2014. Macroscopic fundamental diagrams: a cross-compariosn of estimation methods. *Transportation Research Part B: Methodological,* 62, 1-12.

Lin, J., Ban, Y., 2013. Complex Network Topology of Transportation Systems. *Transport Reviews,* 33**,** 658-685.

Liu, R., May, T., Shepherd, S., 2011. On the fundamental diagram and supply curves for congested urban networks. *Transportation Research Part A: Policy and Practice,* 45**,** 951-965.

Lum, K.M., Fan, H.S.L., Lam, S.H., Olszewski, P., 1998. Speed-flow modeling of arterial roads in Singapore. *Journal of transportation engineering,* 124**,** 213-222.

May, A.D., Shepherd, S.P., Bates, J.J., 2000. Supply curves for urban road networks. *Journal of Transport Economics and Policy* 34**,** 261-290.

Mtoi, E.T., Moses, R., 2014. Calibration and evaluation of link congestion functions: applying intrinsic sensitivity of link speed as a practical consideration to heterogeneous facility types within urban network. *Journal of Transportation Technologies,* 4**,** 141-149.

Nagle, A.S., Gayah, V.V., 2014. Accuracy of networkwide traffic states estimated from mobile probe data. *Transportation Research Record: Journal of the Transportation Research Board,* 2421**,** 1-11.

Ohta, K., Harata, N., 1989. Properties of aggregate speed-flow relationship for road network. Proc. 5-th World Conference on Transport Research 1989 Yokohama, Japan. 451–462.

Ortigosa, J., Menendez, M., Tapia, H., 2013. Study on the number and location of measurement points for an MFD perimeter control scheme: a case study of Zurich. *EURO Journal on Transportation and Logistics,* 3 (3-4) 245-266.

Overgaard, K.R., 1967. Urban transportation planning: Traffic estimation. *Traffic Quarterly,* 21**,** 197-218.

Patriksson, P., 1994. *The traffic assignment problem: models and methods,* Utrecht, the Nertherlands, VSP.

Porta, S., Crucitti, P., Latora, V., 2006. The network analysis of urban streets: a primal approach. *Environment and Planning B: Planning and Design,* 33**,** 705-725.

Sakamoto, Y., Ishiguro, M., Kitagawa, G., 1986. *Akaike information criterion statistics,* D. Reidel Publishing Company, Dordrecht.

Schneider, M., 1963. A direct approach to traffic assignment. *Highway Research Record*.

Shahpar, A.H., Aashtiani, H. Z., Faghri, A., 2011. Development of a delay model for unsignalized intersections applicable to traffic assignment. *Transportation planning and technology,* 34**,** 497-507.

Sheffi, Y.1985. *Urban transportation networks: equilibrium analysis with mathematical programming methods,* Englewood Cliffs, NJ, Prentice-Hall.

Skabardonis, A., Dowling, R., 1997. Improved speed-flow relationship for planning applications. *Transportation Research Record: Journal of the Transportation Research Board,* 1572, 18-23.

Smeed, R.J., 1966. Road capacity of city centers. *Highway Research Record,* 8**,** 455-458.

Smock, R.B., 1963. A comparative description of a capacity-restrained traffic assignment. *Highway Research Record,* 6**,** 12-40.

Spiess, H., 1990. Technical note—Conical volume-delay functions. *Transportation Science,* 24**,** 153-158.

Taylor, M.A.P., 1977. Parameter estimation and sensitivity of parameter values in a flow-rate/travel-time relation. *Transportation Science,* 11**,** 275-292.

Taylor, M.A.P., 1984. A note on using Davidson's function in equilibrium assignment. *Transportation Research Part B: Methodological,* 18**,** 181-199.

Thomson, J.M., 1967. Speeds and flows of traffic in Central London. *Traffic Engineering & Control,* 8**,** 721-725.

Tisato, P., 1991. Suggestions for an improved Davidson travel time function. *Australian Road Research,* 21**,** 85-100.

Tong, C.O., Hung, W.T., Lam, W.H.K., Lo, H.K., Lo, H.P., Wong, S.C., Yang, H., 2003. A new survey methodology for the annual traffic census in Hong Kong. *Traffic engineering & control,* 44**,** 214-218.

Transport Department 2010. The annual traffic census 2010. Traffic and Transport Survey Division, Transport Department, Government of the Hong Kong SAR.

Transportation Research Board 2000. Highway Capacity Manual. *National Research Council, Washington, DC.*

Wardrop, J.G., 1968. Journey speed and flow in central urban area. *Traffic Engineering & Control,* 9**,** 528-532.

Wong, S.C., 1998. Multi-commodity traffic assignment by continuum approximation of network flow with variable demand. *Transportation Research Part B: Methodological,* 32**,** 567-581.

Wong S.C., Du, Y.C., Ho, H.W., Sun L.J. (2003) Simultaneous optimization formulation of a discrete/continuous transportation system. *Transportation Research Record*, 1857, 11-20.

Wong, S.C., Lee, C.K., Tong, C.O., 1998. Finite element solution for the continuum traffic equilibrium problems. *International Journal for Numerical Methods in Engineering,* 43**,** 1253-1273.

Wong, S.C., Sun, S. H., 2001. A combined distribution and assignment model for continuous facility location problem. *The Annals of Regional Science,* 35**,** 267-281.

Wong, S.C., Yang, H., 1999. Determining market areas captured by competitive facilities: a continuous equilibrium modeling approach. *Journal of Regional Science,* 39**,** 51-72.

Wong, W., Wong, S.C., 2015. Systematic bias in transport model calibration arising from the variability of linear data projection. *Transportation Research Part B: Methodological,* 75, 1-18.

Xie, C., Cheu, R.L., Lee, D., 2001. Calibration-free arterial link speed estimation model using loop data. *ASCE Journal of Transportation Engineering,* 127 (6), 507-514.

Xie, D.F., Wang, D.Z.W., Gao, Z.Y., 2015. Macroscopic analysis of the fundamental diagram with inhomogeneous network and instable traffic. *Transportmetrica A: Transport Science*, DOI: 10.1080/23249935.2015.1094535

Yang, H., Wong, S.C., 2000. A continuous equilibrium model for estimating market areas of competitive facilities with elastic demand and market externality. *Transportation Science,* 34**,** 216-227.

Yang, H., Yagar, S., Iida, Y., 1994. Traffic assignment in a congested discrete/continuous transportation system. *Transportation Research Part B: Methodological,* 28B, No.2, 161-174.

Yin, J., Wong, S.C., Sze, N.N., 2012. Optimization of housing allocation and transport emissions using continuum modeling approach. *Asian Transport Studies,* 2**,** 93-108.

Yin, J., Wong, S.C., Sze, N.N., Ho, H.W., 2013. A continuum model for housing allocation and transportation emission problems in a polycentric city. *International Journal of Sustainable Transportation,* 7**,** 275-298.